Arab Gulf J. scient. Res. **3** (2), pp. 513-537 (1985)

Reservoir Delineation within the Abu Madi Gas Field, Nile Delta, Using the Seismic Inversion Technique

Y.E. Abd Elhadi

College of Education Umm El-Qura University
Makkah al-Mukarramah, Saudi Arabia

ABSTRACT. The seismic inversion technique is a relatively novel method in exploration geophysics. The present paper discusses the methodology of this technique and illustrates its application to a specific problem in hydrocarbon exploration. The seismic inversion technique was applied in a recent digital seismic survey in the Abu Madi Gas Field, Egypt, in an attempt to delineate the reservoirs in that field and optimize their development.

High frequency as well as high amplitude seismic responses characterize thin gas-filled lenses, while low frequencies and high amplitudes characterize thick sand lenses. The wavelet processes section demonstrated that the Abu Madi Formation is characterized by rapid lateral lithofacies changes which are related to the fluvio-deltaic depositional environment of these rocks. The wavelet-processed sections also showed that amplitude anomalies, which may be significant in terms of hydrocarbon potential, exist at deeper levels (Sidi Salem). Subsequently, deeper drilling has led to the discovery of new reservoirs for gas and condensate accumulations.

Detailed velocity analysis from seismic data yielded highly stable velocity curves. The same results are observed in the borehole velocities. This indicates lithostratigraphic uniformity in the Abu Madi sedimentary section.

It is expected that seismic data collected with optimum unified-field parameters with increased high frequency content can provide even more useful results.

The Abu Madi Gas Field is located in the northeast corner of the Nile Delta. Seven exploratory wells have been drilled so far (between 1969 and 1979), five of which produced from the Abu Madi Formation while the other two were abandoned as unproductive.

The field has been surveyed by aeromagnetic and gravity methods and by numerous seismic surveys. The conventional structural interpretation of the geophysical data did not delineate the reservoir in sufficient detail for estimating

the volumetric gas reserves because the reservoir is stratigraphically controlled. Since the produced gas is used in a fertilizer plant, development of the field became an urgent objective.

The Abu Madi Field, which has a surface area equal to 200 km^2, is located onshore in the northeast corner of the Nile Delta (Fig. 1). The geologic setting of the field was evaluated in the light of knowledge of the geology of the entire Delta, integrated with the available geophysical data, which included magnetic, gravity, analog seismic and modern (digital) seismic surveys. Six digitally recorded seismic lines (Fig. 2) were selected for reprocessing using the advanced wavelet processing

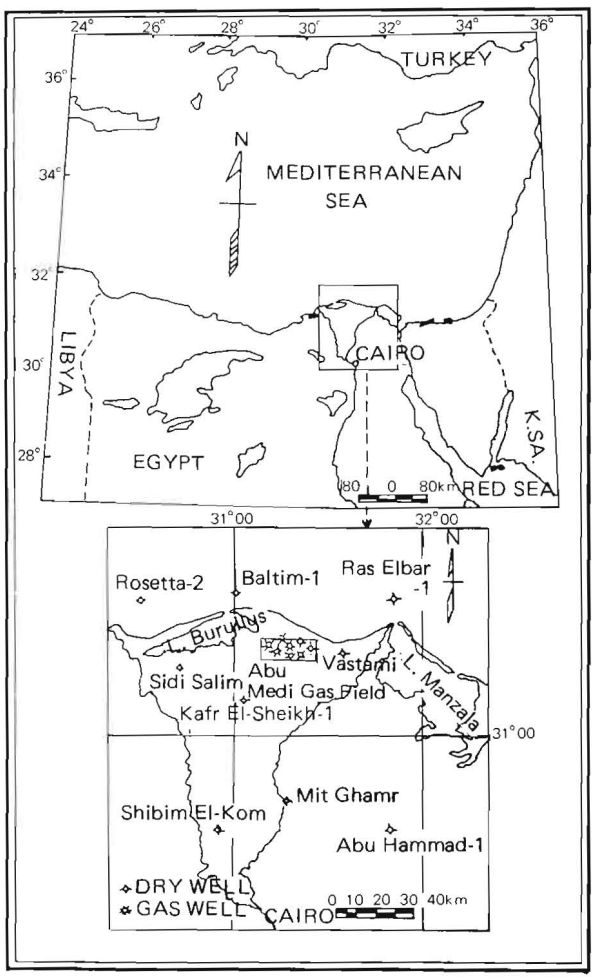

Fig. 1. Location map of Abu Madi field.

technique with 20 data improvement, where acoustic impedance, time, and depth sections were derived from the conversion of the enhanced seismic traces (in the form of pseudo-reflection coefficient time-series). The velocity analysis and velocity measurements from the deep wells in the field were also used. In the inversion process, a deterministic approach was used to compute a model of the propagating wavelet from the characteristic curves of the receivers plotted by the manufacture (Fig. 3-4). From these curves a direct operator was extracted as a two-sided, time domain zero-phase wavelet (Fig. 5) which was used as a prestack deconvolution operator. The aim was to make the effective wave shape the same for all the traces that were to be stacked together to avoid attenuation of the stacked signal, since individual traces generally are phase-shifted, especially in high frequency zones. Prestacked deconvolved traces closely approached the reflectivity time-series of the subsurface layers. The latter were computed at 2 msec and 4 msec sample intervals, and interval velocities were computed for each sample.

The computed interval velocities were always checked against the velocities measured in the deep wells from calibrated sonic logs and they were always within the limits of confidence. The thickness of gas bearing zones in the Abu Madi Formation approaches 135 m in a few localities, but is generally thinner. Subsurface information indicates that the gas-bearing zones are constituted of discrete sand

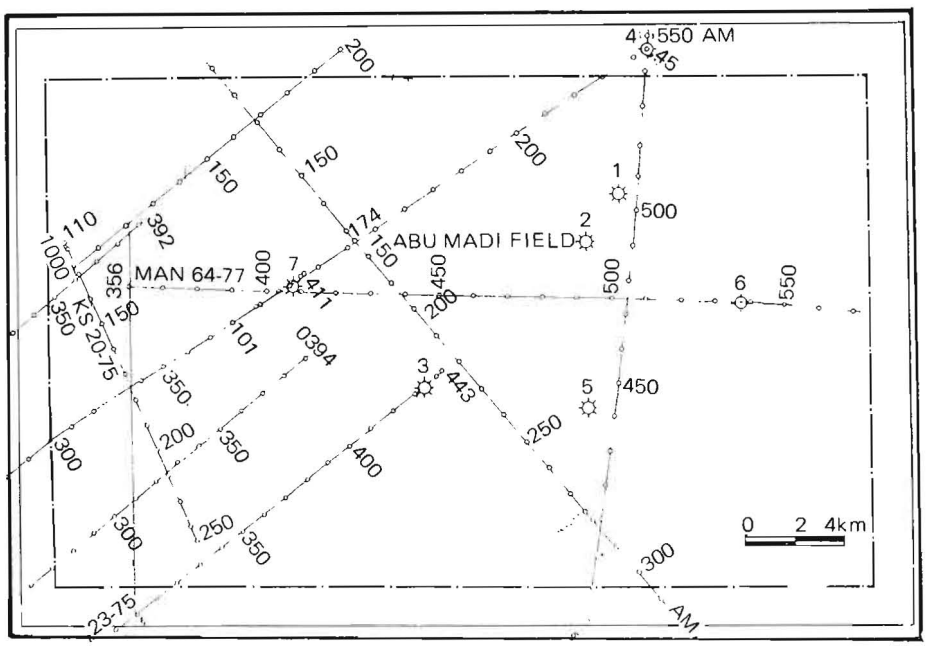

Fig. 2. Index map of seismic lines

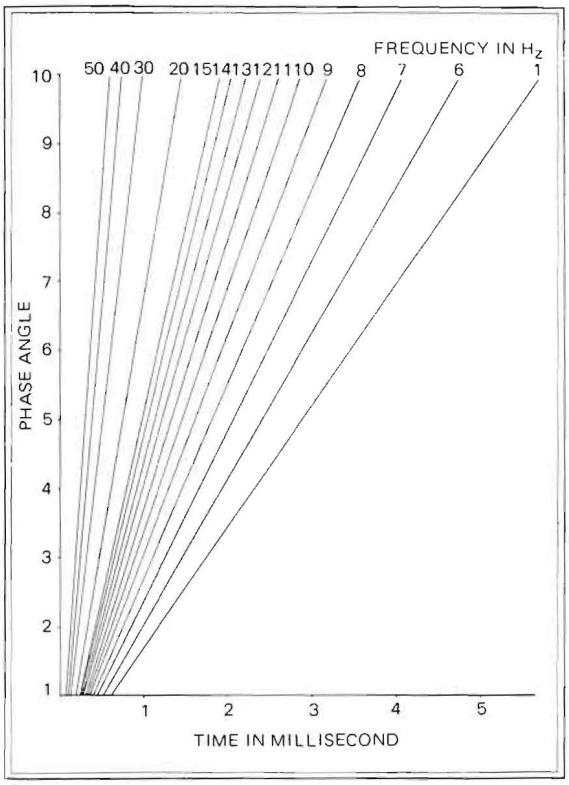

Fig. 3. The phase-frequency response curves.

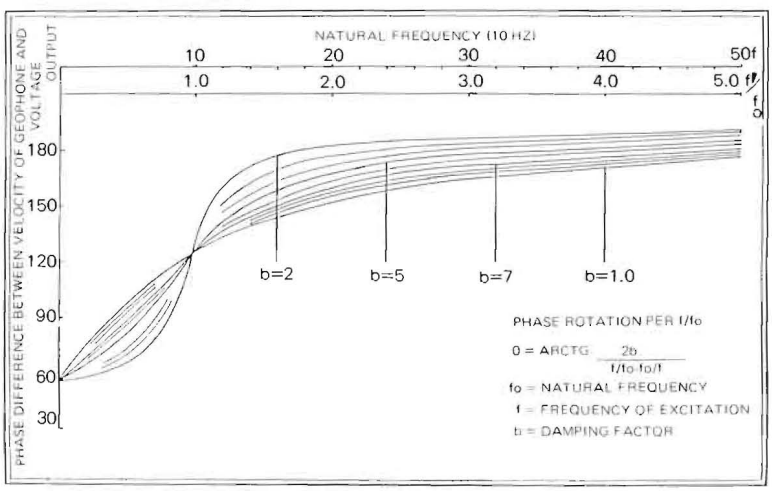

Fig. 4. The time-phase relation per frequency from 5 H_z to 50 H_z.

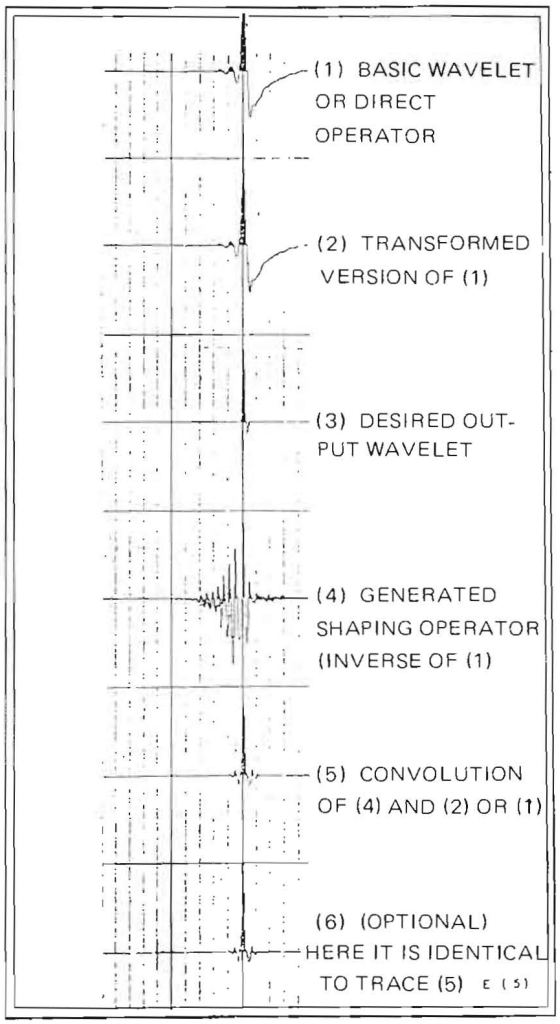

Fig. 5. A trial of wavelet extraction and shaping on line KS-23-75.

lenses rather than forming a well-defined continuous reservoir. These discrete sand reservoirs are expressed on the wavelet processed and acoustic impedance sections as amplitude anomalies that possess valuable lateral extension (Berquey *et al.* 1974). The nature of these sand lenses explains why some wells are better producers than others (Fig. 6).

The main geological objective established in the study area was the determination of the distribution of the sand lenses within the basal Pliocene (Abu Madi Formation).

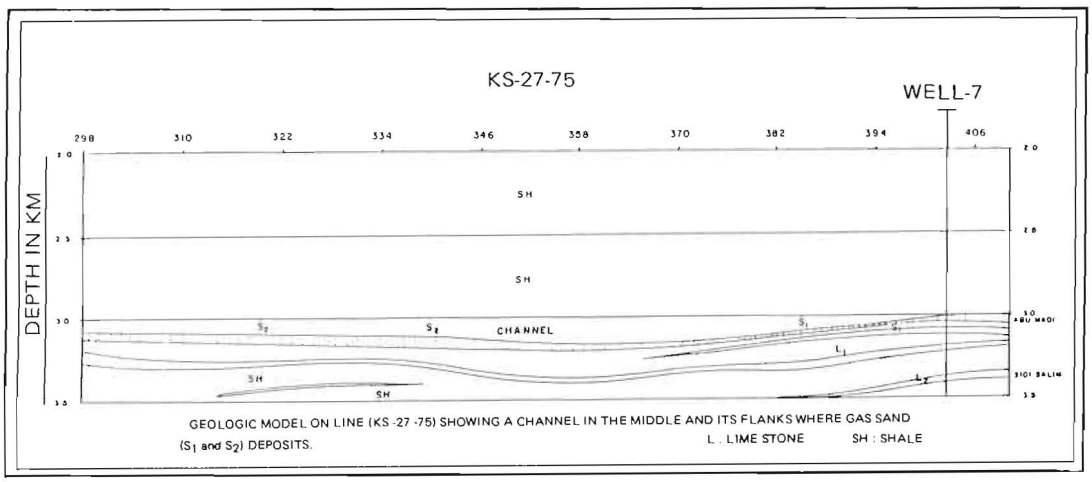

Fig. 6. Transfer seismic data to geological model.

Regional Geologic Setting

The study of the geology of the area under investigation depends wholly on subsurface information. More than twelve exploratory wells have been drilled in the delta region. These wells have penetrated rocks ranging in age from Jurassic to Recent. The depth of the basement rocks increases northwards (Abd Elhady 1979). Accordingly, the sedimentary section becomes thicker to the north. Wells drilled in the study area did not reach rocks older than Miocene. The basement depth is estimated from magnetic surveys to vary from 2000 m in the south to more than 10,000 m in the north of the Delta (Korrat 1977).

A thin Jurassic section (53 m) in the Delta region was encountered in the Shebin El-Kom-1 borehole (Fig. 7). The thickest Jurassic succession in Egypt was penetrated in the Abu Hammad Well-1 (East of the Delta). Cretaceous was also penetrated in Shebin El-Kom, where 869 m of sands, sandstones and shales represent the Upper Cretaceous, and 545 m of limestone represent the Lower Cretaceous. Paleocene deposits have not been recorded in any well in the Delta so far, but the Eocene was penetrated in both the Shebin El-Kom and Mit Ghamr wells. Eocene exposure are present along the southern parts of the Delta.

The surface evidence indicates periodic movement along the E-W 'hinge-line' (Fig. 7) during time of the depositional history. From the lithofacies distribution, an open sea environment is postulated to the north of the 'hinge-line' and a shore line to the south and near the hinge, especially in the eastern part of the Delta region. A significant change in shelf gradient near the hinge may have created conditions favourable for a carbonate barrier (reef) to develop.

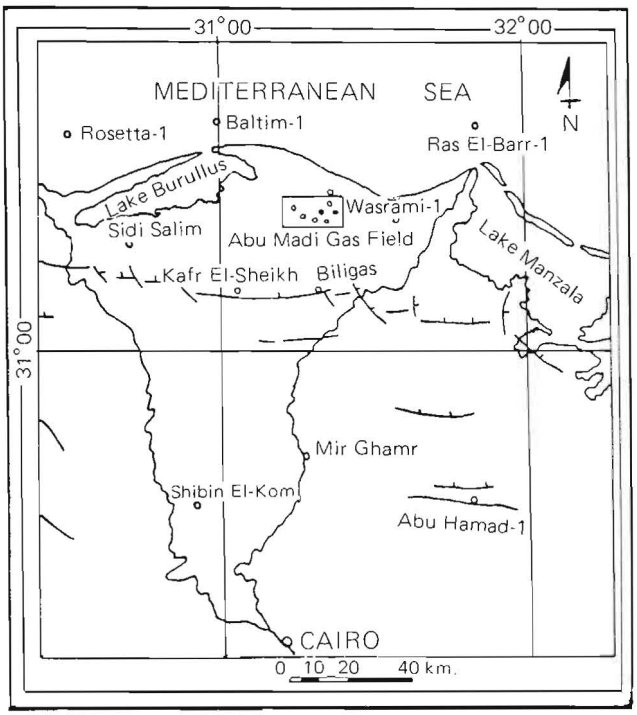

Fig. 7. Hinge line fault distribution in Nile Delta area.

Towards the south, near-shore conditions, behind the postulated carbonate barrier, enabled some clastic or carbonate sand bars to be formed which constitute potential reservoir rocks. During Upper Eocene deposition, northward tilting or subsidence lowered the area forming the northern edge of the Nile Delta.

The Oligocene period brought a large accumulation of fluvial to estuarine sediments into northern Egypt, where they transgressed northwards over older sediments. Within the mid-delta region, Oligocene sands and shales are inter-bedded, and form good reservoir and caprock combinations.

Oligocene formations are overlain by a thick section of Miocene and Pliocene deltaic to marine deposits which is penetrated in the Nile Delta wells. This sequence is overlain by a thin succession of Quaternary shallow marine deposits. The latter generally dip towards the north, as indicated by drilled wells and N-S seismic lines. Due to the huge thickness of the Mio-Pliocene in the north of the Delta, no older formations were reached in the Abu Madi wells. The Mio-Pliocene succession consists mainly of shale with minor alternations of sands and a few anhydrite beds ranging from shallow marine to fluvio-marine environments, with short intervals of enclosed lagoonal conditions. Uplift at the close of the Oligocene period exposed Lower Miocene sediments at the south edge of the Nile Delta.

It is difficult in the subsurface to determine a boundary between the Middle Miocene rock units and the underlying or overlying units. The upper boundary was arbitrarily taken at a recognizable seismic event which indicates a channelled unconformable surface.

The whole succession has been divided by Rizzini *et al.* (1976) from top to bottom into the following rock-units (Fig. 8).

Recent	Bilqas Formation
	Mit Ghamr Formation
	Baltim Formation
Upper Pliocene	Al-Wastani Formation
	Kafr El-Sheikh Formation
Lower Pliocene	Abu Madi Formation

Unconformity

Middle Miocene	Sidi Salem Formation
Lower Miocene	Pre-Sidi Salem Formation

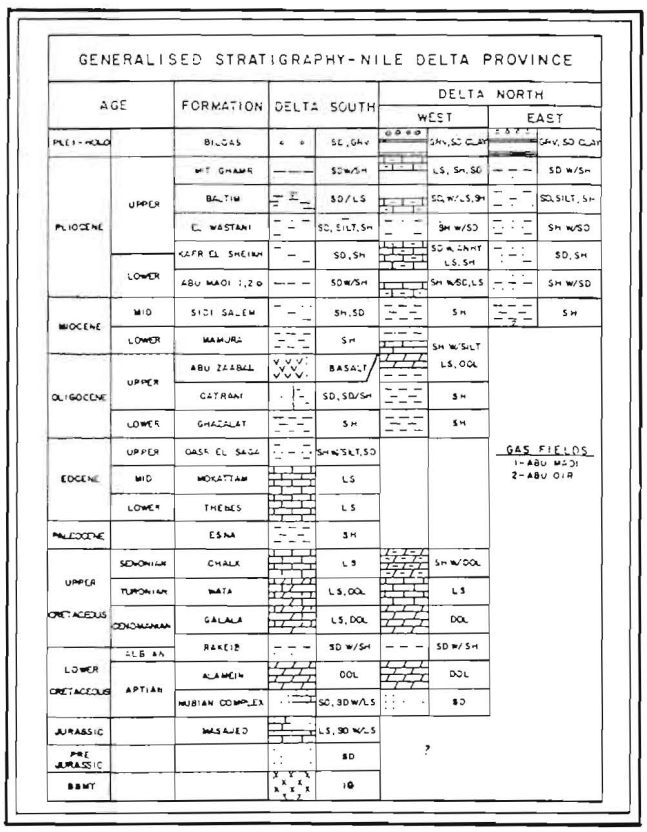

Fig. 8. Generalised stratigraphic table for Nile Delta province.

The Sidi Salem Unit is of shallow marine and/or deltaic origin, and sometimes indicative lagoonal conditions.

The post-unconformity 'Abu Madi' Formation, which corresponds to Messinian time, and rests unconformably on the Sidi Salem Formation (based on facies changes and without paleontologic evidence). It is of particular interest, being the most promising formation in the Delta basin since gas discoveries were proved within its porous sand deposits.

The Abu Madi Formation is characterized by rapid lateral lithofacies changes characteristics of its fluviodeltaic environment of deposition. It constitutes the Lower Pliocene and commences with coarse basal sands, followed by a sequence of interbedded sands and shales which passes upward rapidly into marine sediments. This Formation has a maximum thickness of about 500 m in the Kafr El-Sheikh Well-1 (Fig. 7) and shows a northward regional dip.

The Kafr El-Sheikh Formation consists of a thick shale sequence with thin sand streaks. It attains its maximum thickness (1700 m) in the Abu Madi field.

The El-Wastani Formation is Pliocene in age (probably Late Pliocene) and is represented by interbedded sands, shales and clays of estuarine and marine origin with a thickness that ranges from 200 to 300 m.

The Baltim Formation overlies the El-Wastani Formation and consists of sands and gravels of fluviomarine origin. It underlies the Bilqas Formation which is represented by very coarse grained sands and gravels with abundant shell fragments formed in a shallow marine environment.

In summary, the geological sequence recognised is mainly composed of shales (source), sands (reservoir) and conglomerates. The sand lenses of basal Pliocene age (the Abu Madi Formation) are the main exploration objective. The unconformity between the Middle Miocene and Pliocene has been penetrated and has been found to be of good hydrocarbon potential. It is expected that the Middle Miocene sediments may also provide good stratigraphic traps. The main geologic features are sand lenses and channel sandstones that constitute ideal stratigraphic traps with good lateral and top seals.

Description of Seismic Data

The area was already covered by magnetic, gravity and analogue seismic surveys. A few digitally recorded lines were acquired in 1975, 1977 and 1979. These multichannel – common depth point (CDP) (Marrand Zagst 1976) seismic reflection lines were shot by using the same recording instrument, an instantaneous floating point recording station (model SERCEL 338 B). The coverage of the survey was 12-fold. While the same recording instrument was used, field parameters were highly variable, rendering the data to some extent inhomogeneous. De-

LINE / PARAMETER	KS-23-75	KS-27-75	AM-001-79	AM-002-79	MAN-64-77	MAN-401-79
Type of spread	End-on	End-on	Split-spread	Split-spread	End-on	Split-spread
Configuration of spread	0-720-3540	0-720-3540	0-450-2475	0-450-2475	0-375-3900	0-450-2475
Off set	720	720	450 & 375	450 & 375	375	450 & 375
Trace Interval	60	60	75	75	75	75
No of Geophones	12/7 & 24/7	12/7& 24/7	24/7	24/7	24/7	24/7
Geoph. array configuration	Two-lines & (tapered)	Two-lines & (tapered)	Parallogram (tapered)	Parallogram (tapered)	Parallogram (tapered)	Parallogram (tapered)
Shot hole pattern	Single hole	3 in line	5 in line	5 in line	7 in line	5 in line
Shot hole depth	12m	6m	6m	6m	6m	6m
Shot hole Interval	—	20m	20m	20m	20m	20m
Length of geoph. array	35 & 77m	40 & 77m	77m	77m	77m	77m
Length of shot hole pattern	—	60 m	80m	80m	120m	80m
Max. length of the spread	3540	3540	2475	2475	3900	2475

Tabel 1

tails of the field techniques are displayed on Table 1. The six seismic lines have been selected according to their proximity to the wells in the area (Fig. 2) to be reprocessed through a wavelet processing sequence to produce true-amplitude (wavelet) and acoustic impedance sections. The zone of interest lies on the seismic sections between 2.5 seconds and 3.0 seconds of two-way reflection time. No multiple reflections were observed on the sections because the subsurface is composed of homogeneous isotropic layers with very weak lithologic contrasts. Some diffraction events, that originated from the terminations of the acoustic impedance boundaries of sand bodies in the basal Pilocene, were recognized, since they differ in shape and form from the primary events.

Wavelet Processing

The signal enhancement of the seismic data was accomplished through a deterministic approach to compute a deconvolution operator for prestack wavelet processing (subsurface dephasing system).

Application of that deconvolution operator (Burns 1968) to seismic traces eliminated the phase distortions caused by the near-surface effects. Since the basic wavelet (signature) was not measured in the field it was computed from the characteristic curves of the geophones. The different steps for the determination of the deconvolution operator are shown in Fig. 9. The output wavelet from this stage (trace 5) is designed to be a band-limited, zero phase wavelet. The second key step was the application of the preprocessor on the CDP trace gather, initial processing must be with amplitude preservations. The preprocessor first rearranges the input trace sequential data into a common depth points format, each trace with a header containing the basic information.

A distance-dependent spherical divergence and an elastic attenuation factor was applied to keep the amplitude characteristics on a given reflecting horizon uniform along the final section.

The third step was a frequency domain deconvolution before stacking to eliminate any short path (peg-leg) multiples.

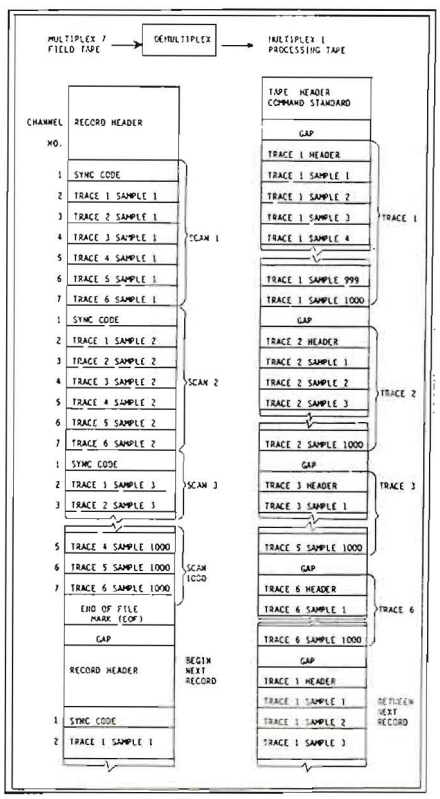

Fig. 9. Deconvolution operations flow chart.

Subsequently, the processing sequence consisted of velocity analysis, field statics, automatic statics (surface consistence method), stacking with relative amplitude preservations, time varying equalization, time varying filter and finite difference wave equation migration. The flow diagram of the wavelet processing is shown in Fig. 10.

Having enhanced the data, a zero-phase wavelet was extracted for a post-stack deconvolution with the aim of contracting the seismic pulse and increasing the frequency content to obtain good resolution. The determination of the wavelet was checked through a comparison of the seismically obtained acoustic impedance traces at a well location with the acoustic impedance derived from the recorded sonic and density logs in that well, provided that the log-derived acoustic impedance log could be regarded as representative of the formation encountered by the seismic signal (virgin formation).

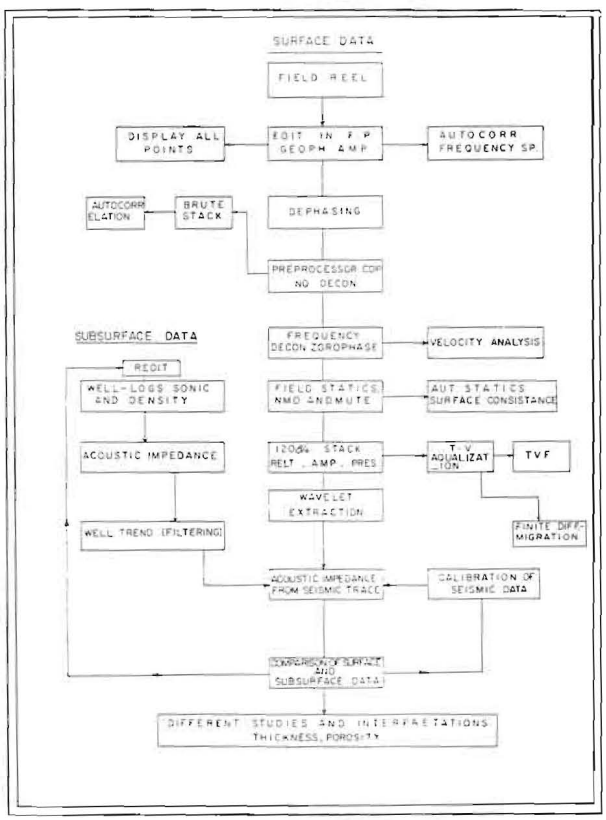

Fig. 10. Flow chart for the special processing of Abu Madi seismic data.

In many cases, sonic and density logs were re-evaluated and it was found that log-editing was necessary. The discrepancies between seismic impedance and borehole log was found to be due to the following deficiencies.

1. Wash out and invasion effects. This is due to soft shales that are caved, eroded and swelled by water absorption and mud infiltration. Typical log responses in such a case involve cycle-skipping and inaccurate time values.

2. Improper data handling.

3. Formation alteration effects.

4. Deviations in the hole. Computation of the post-stack deconvolution operator function was performed through a window corresponding to the gas-bearing zone (basal Pliocene) after adding the low-frequency component from the velocity analyses to obtain absolute acoustic impedances and make these equivalent to the log-derived acoustic impedances.

To obtain a quick and satisfactory match within the selected window, a scaling function was applied in order to attenuate or reinforce parts of it. In cases of poor matching, the operator function was recalculated and all parameters involved in both data-sets (seismic and well logs) were checked until the errors were reduced.

Three types of output data result from the post-stacking wavelet processing:

1. A high resolution zero-phase wavelet processed section for each conventional seismic section.

2. The reflectivity time-series in these wells to which the seismic sections were tied.

3. The best wavelet form that provides a satisfactory match between surface and subsurface data.

Inversion Velocity and Basic Logs

Seismic data were recorded at a low-cut frequency equal to 8 Hz, to avoid ground roll. For accurate correlation between seismic traces and sonic log data, this low-frequency band was added to the seismic traces in order to avoid phase differences. Where the geologic section consists of a flat homogeneous mass of shale, it does not show any significant lateral variation in the seismic velocity differences between velocities computed in boreholes and those derived from the velocity analysis of seismic data.

Therefore, the vertical average velocities derived from velocity analysis were converted into reflectivity series, in terms of both time and depth. Reflectivity time-series were then used in the construction of the wavelet-processed sections (with relative amplitude preservation), while the reflectivity depth series were

employed to construct the depth sections (Shariff 1975). Correct polarity determination was accomplished through comparison of the calibrated sonic logs and filtered seismic traces.

A constant density value of 2.4 gm/cm^3 was assigned to intervals which were not logged for density in order to compute acoustic impedance values from the measured velocities.

The Seismic Inversion

The aim of wavelet-processing prior to seismic inversion was to enhance the seismic data and obtain the reflectivity series, the wavelet and the wavelet-processed sections. In addition, this technique involves preparing the data to be inverted from wavelet-processed sections into acoustic impedance sections that match closely the actual subsurface geologic model and provide an estimate of the lithologic properties of the layers within the earth.

The subsurface model for the layered earth is assumed to consist of a series of plane-homogeneous layers, each being characterized by its specific acoustic impedance (Z_i).

Through that layered system the CDP-stacked and migrated seismic trace represents a normal incidence plane-wave whose response for the sub-surface model approximates a one-dimensional, band-limited reflection coefficient time-series. In wavelet processing, we separate the earth's reflectivity from the seismic wavelet which, when convolved together, provides a seismic trace that is generally contaminated with noise. The convolutional model is shown in Fig. 11.

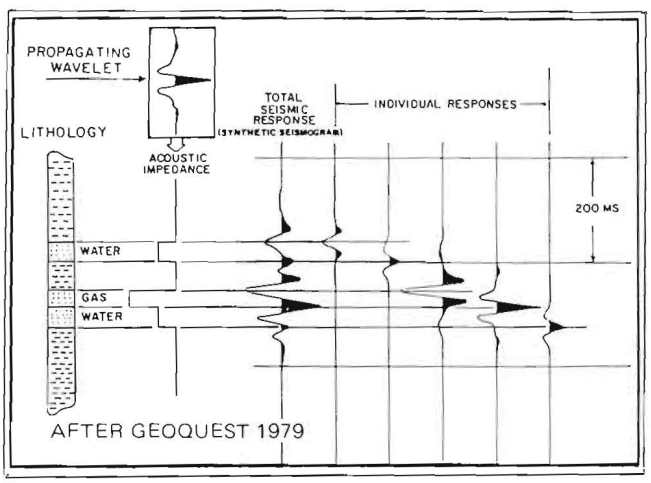

Fig. 11. Standard method for the convolution operations (After Geoquest 1979).

Inversion was achieved through acoustic impedance sections in terms of both time and depth, where amplitude anomalies were more pronounced and the vertical resolution and lateral definitions were increased.

Basic of the Stratigraphic Interpretation

Thin sand beds (less than one quarter wave length) encased in shale or interbedded with shale give a seismic response that varies in amplitude, but not in shape or character with thickness (Schramm *et al.* 1977).

Consequently, the thickness of a thin sand bed can be measured from the amplitude of its seismic response with a degree of net thickness resolution which is superior to that obtained from a timing measurement. Moreover, experimental results (Gregory 1976) and field data (Tatham and Stoffa 1976) have demonstrated that gas-filled rocks have much lower velocities and, therefore, greater acoustic impedance contrasts than those displayed by either oil- or brine-saturated rocks. Thus, gas filled rocks, especially sands, reflect a greater proportion of the incident energy, and the amplitude anomalies associated with gas/brine contacts are always greater than those related to oil brine interfaces (Demenico 1976, 1977).

Polarity reversals, also characterizes, the reflection coefficients at the upper and lower interfaces of a gas-filled sand encased in a shale of higher velocity. The upper one will be negative ($Z_2 - Z_1 < 0$) while the lower one will be positive ($Z_2 - Z_1 > 0$), Z being the acoustic impedance. Moreover, it was also observed that very thin sand beds are characterized by very high frequency decreases with increasing thickness, of the sand bed. Thus, frequency can be considered as a guide to both the presence of gas and the approximate volume of its reservoir. Thus, amplitude and frequency anomalies were used to obtain quantitative estimates of gas-filled sand lenses and in planning for optimum development of the field. These

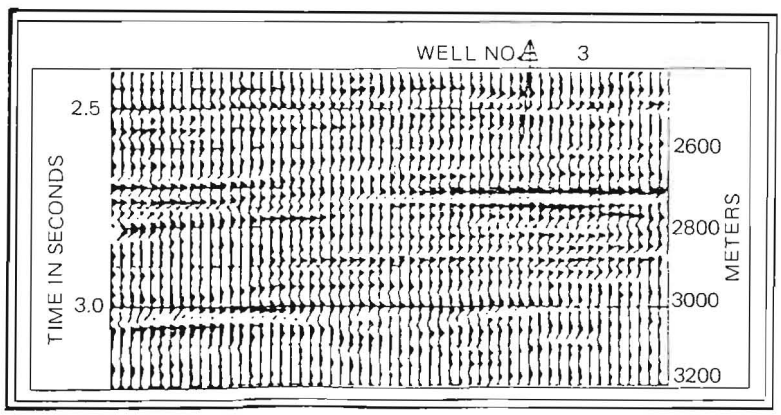

Fig. 12. The wavelet processed line KS-23-75 (for location, see Fig. 2).

properties also provide reliable information concerning the reservoir model, and specifically lithology, the net way thickness and the identification of gas/fluid and fluid/fluid contacts.

Amplitude Anomaly Examples

The wavelet-processed line K5-23-75 (Fig. 12) passes close to the producing well AM-3, which lies near shot point 435 (See also Fig. 2).

The pay zone occurs at a reflection time of 2.7 sec (3100 m) and consists of a gas-filled sand reservoir with a thickness of about 125 m. It appears as a very strong

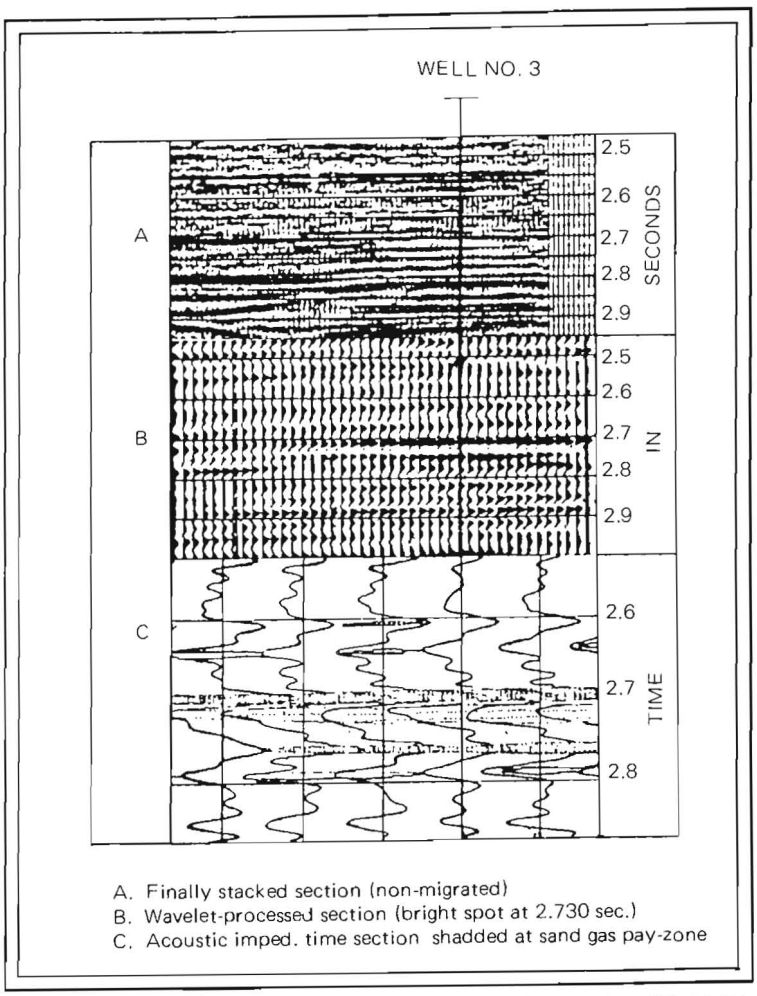

Fig. 13. Three versions of the same seismic section on line KS-23-75.

amplitude anomaly (bright spot) which extends to the left for a distance of about 20 shot points and extends to the right to a point beyond the end of the displayed line. No structural element is observed; only a very gentle dip towards the left. The sand/shale ratio seems to increase with dip and is demonstrated by a weakness in amplitude. Another technique of illustrating the phenomenon is shown in Fig. 13, where three versions of the same section are presented. At the top there is a finally stacked, non-migrated section; in the middle the wavelet-processed section already discussed; and at the bottom an acoustic impedance section, expressed in terms of time and with the gas-filled sand section shaded. The correlation of the seismic response of the gas reservoir with lithology and sonic data in the well AM-3 is shown in Fig. 14.

A similar mode of correlation between surface and subsurface data at well AM-No.7 is shown in Fig. 15.

The two wells AM No. 1 and AM No. 2 are near but offset from line MAN-401-79. Both show a pay zone below 3230 m that matches very well with the acoustic impedance depth sections.

To map the amplitude anomalies on the different sections for correlation purposes, amplitude anomalies are measured and recorded on different zones (Fig. 16).

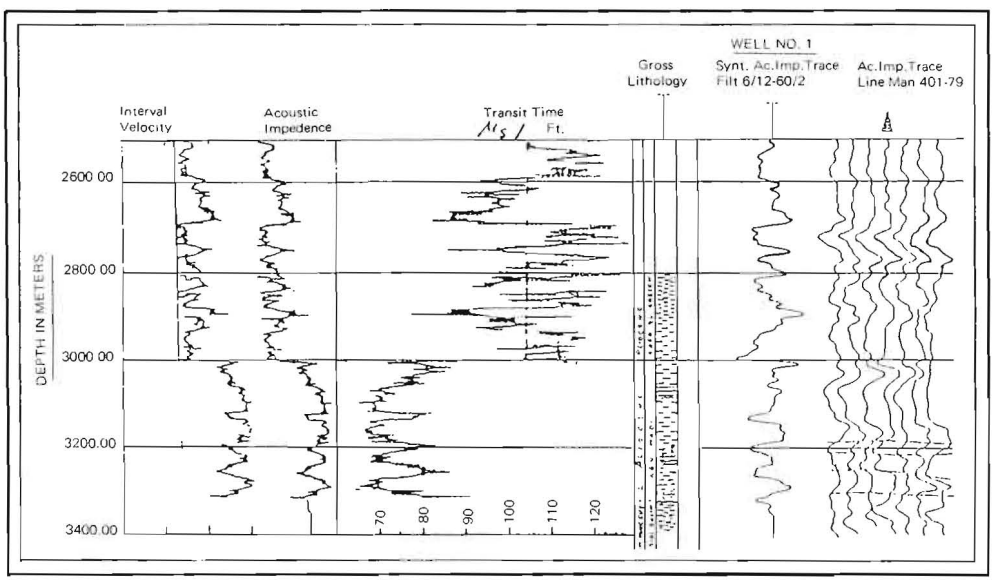

Fig. 14. The correlation of interval velocity, acoustic impedance, transit time, lithology and synthetic acoustic impedance traces in Well no. 1.

However, it is possible to dispense with these maps when the amplitude anomalies are clear on the wavelet processed sections. This was the case in choosing a location for well AM No. 8, which was proposed at shot point 198 of the wavelet-processed section AM-1-79 (Fig. 17). The well is now producing from a gently-dipping amplitude anomaly (at a time of 2.7 sec) from the Abu Madi basal Pliocene Formation. It is interesting to compare the wavelet-processed sections at producing and a non-producing wells to estimate qualitatively and quantitatively the corresponding amplitude anomalies. A comparison of the amplitude anomaly on Fig. 17 with that at the dry well AM No. 4 on line MAN-401-79 reveals a big difference (Fig. 18). It is clear from figures 19 and 20 that acoustic impedance and velocity logs are helpful in correlation of such pay-zones.

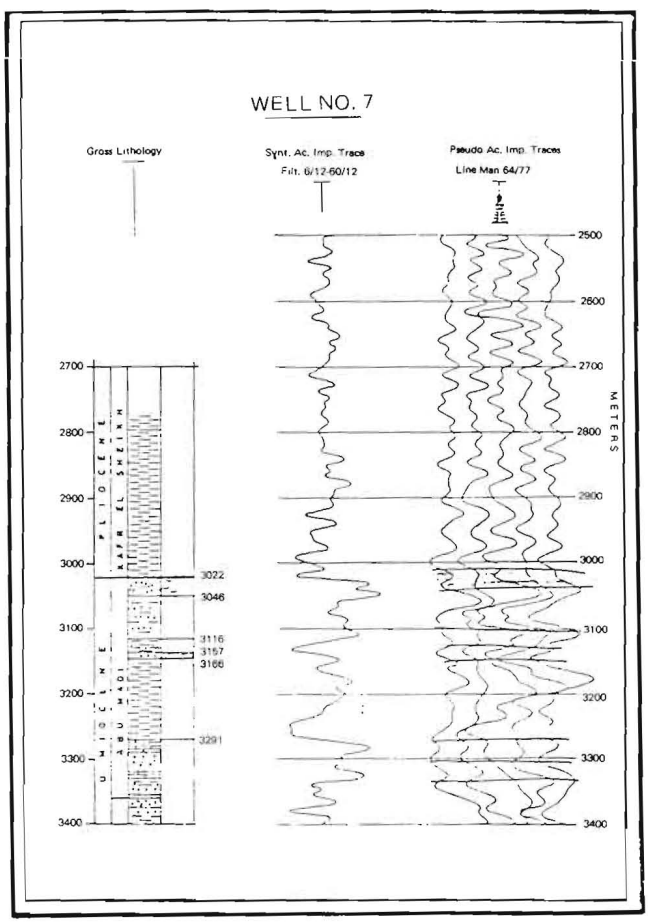

Fig. 15. Correlation between surface and subsurface data at Well no. 7.

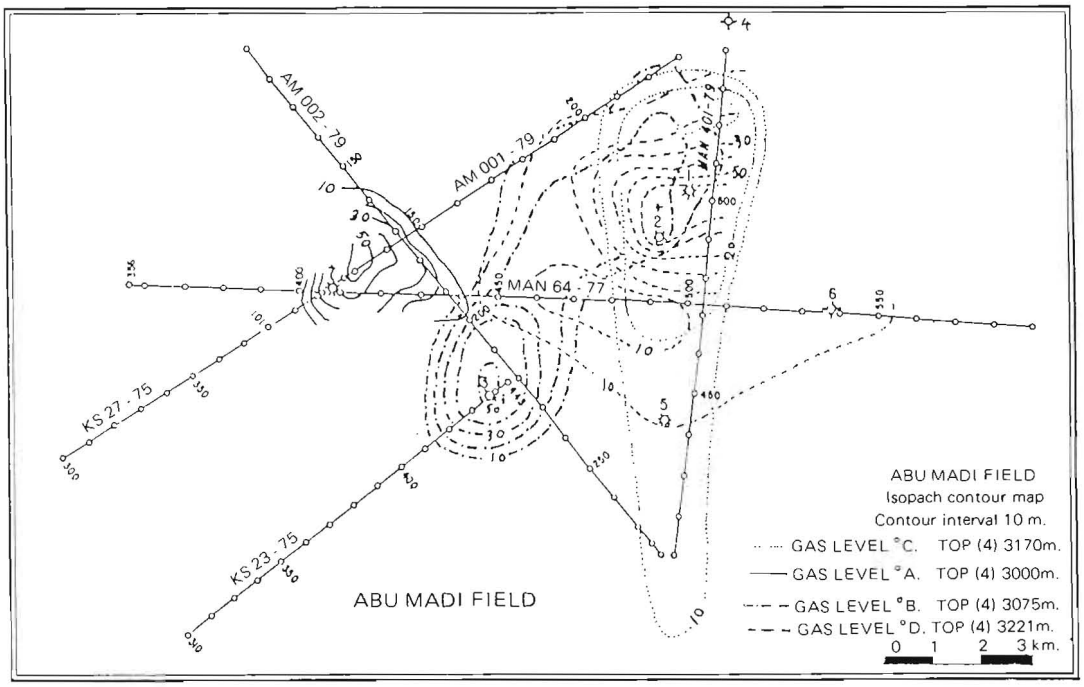

Fig. 16. Isopach contour maps of different gas levels in the Abu Madi field.

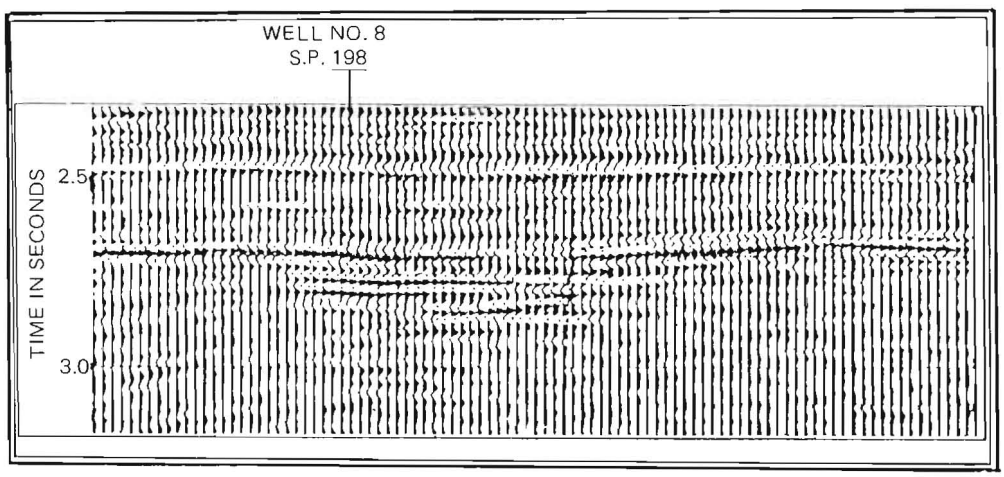

Fig. 17. Processed section AM-1-79 and location of Well AM-no. 8 (bright spot). Profile = 1.4 km

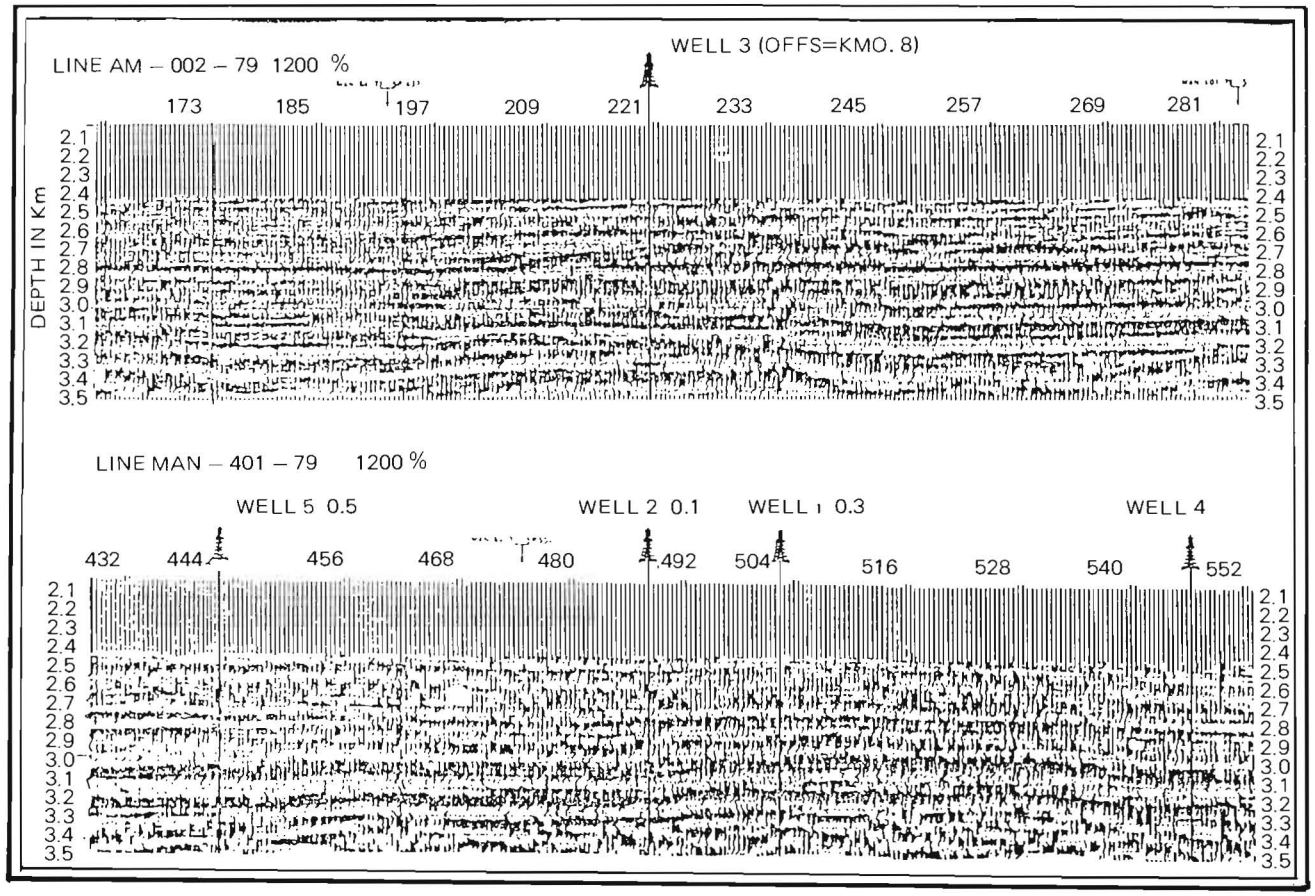

Fig. 18. Amplitude correlation across Wells no. 3, 5, 2, 1 and 4.

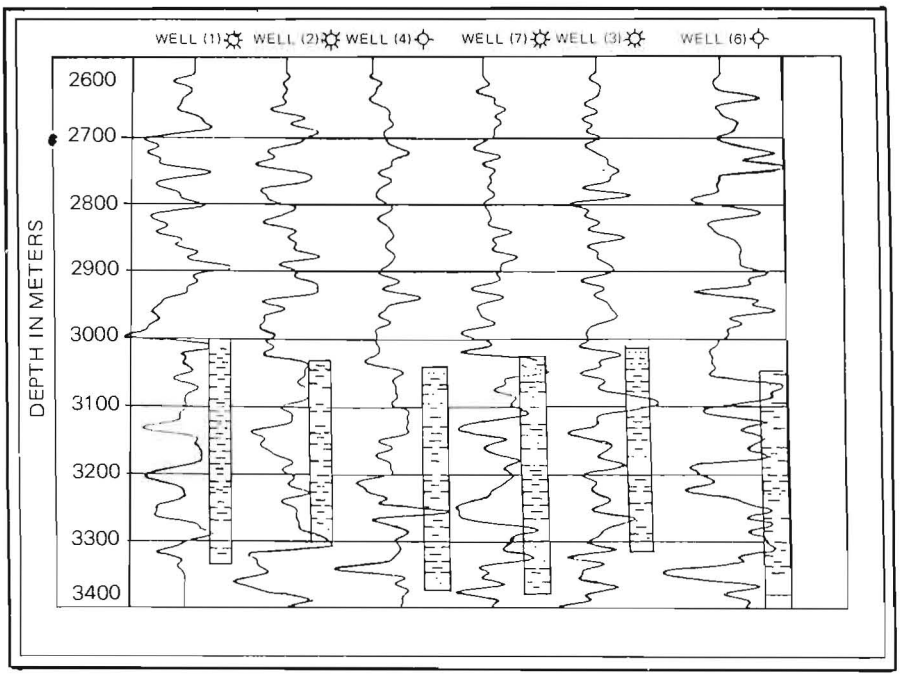

Fig. 19. Comparison of acoustic impedance logs in the Abu Madi field.

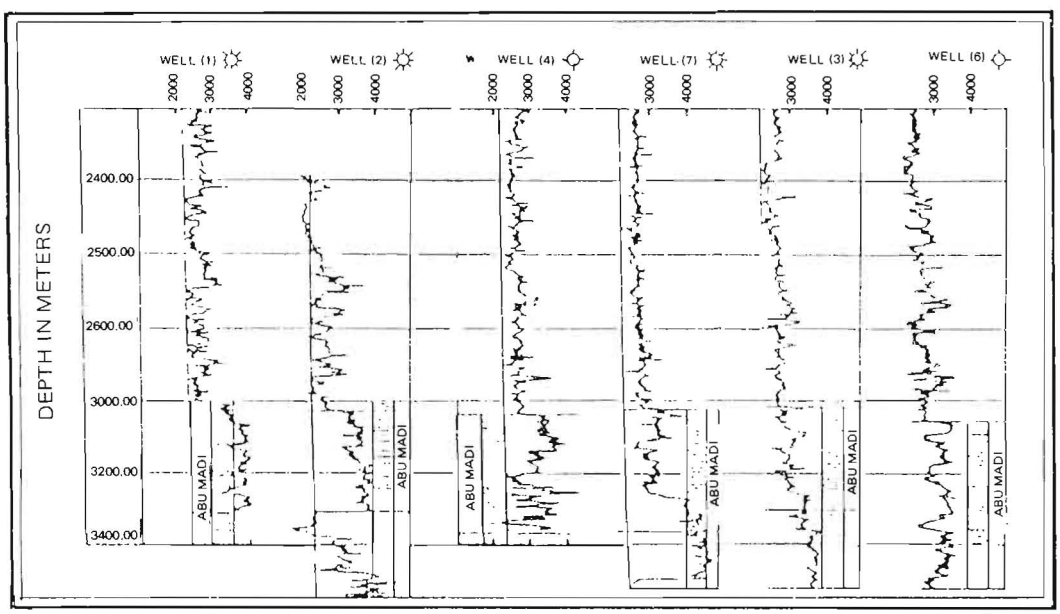

Fig. 20. Comparison of velocity logs in the Abu Madi field.

Conclusion

The development of the Abu-Madi Gas Field using the seismic inversion technique has led to the following conclusions:

1. For sand reservoirs encased or interfingered within shale, seismic inversion is an effective technique in hydrocarbon detection, irrespective of the absence of any tectonic structures.

2. Wavelet-processing for seismic data, gathered with optimum field techniques, can result in a good source of reliable information that helps in the appraisal and development of both new and producing gas fields.

3. Synthetic seismograms and seismic data must be processed by the same wavelet operator function in order to obtain a good match between them.

4. A lack of matching between synthetic seismograms and seismic data is not necessarily attributable to errors in either of these (such as insufficient calibration or adjustments to offsets) because there are so many parameters involved in the data production.

5. In addition to their value in stratigraphic interpretation, wavelet-processed sections can also help to delineate structural elements, including minor regional dips.

6. The wavelet-processed section showed that the Abu Madi Formation is characterized by rapid lateral changes in lithofacies which are believed to be related to an original fluvio-deltaic environment.

7. Detailed velocity analysis from seismic data yielded relatively stable velocity curves. The same results are observed in the borehole velocities. This indicates a uniformity in the Abu Madi sedimentary section.

8. It is expected that seismic data collected with optimum unified field parameters with an increased higher frequency content would provide even more useful results.

9. High frequencies, as well as high amplitudes, characterize thin gas-filled lenses, while low frequencies and high amplitudes characterize thick sand lenses.

10. The wavelet-processed sections show that higher amplitude anomalies, which may be of hydrocarbon potential, exist in deeper horizons (Sidi Salem Formation). Therefore, deeper drilling may lead to new reservoirs for gas and condensate accumulations.

References

AbdEl Hady, Y.E. and **Tealeb, A.** (1979) Thickness of the earth's crust in north Egypt and the east Mediterranean, *The 24th International Geophysical Symposium Cracow, Sept. 4-7, Poland.*

Becquey, M., Lavergne, M and **Willm, C.** (1974) Acoustic impedance log computed from seismic traces, *Geophysics* **44**: 1485-1501.

Burns, W.R. (1968) A statistically optimized devolution. *Geophysics* **33**: 255-263.

Demenico, S.N. (1976) Effect of brine gas mixture on velocity in unconsolidated porous and reservoir, *Geophysics* **41**: 882-898.

Demenico, S.N. (1977) Elastic properties of unconsolidated porous and reservoirs, *Geophysics* **42**: 1339-1368.

Geoquest, J.F. (1979) An investigation into discrepancies between lithology, propagating and seismic response. *Schlumberger technical services Inc.* Singapore, 181-205.

Gregory, A.R. (1976) Fluid saturation effects on dynamic elastic properties of sedimentary rocks. *Geophysics* **41**: 895-921.

Korrat, I.M.I. (1977) *Geophysical Studies on Some Subsurface Formations in the Nile Delta Region*, M.Sc. Thesis faculty of Sci., Mansoura Univ., Mansoura, Egypt.

Marr., J.V. and **Zagst, E.F.** (1976) Exploration horizons from new seismic concepts of CDP and digital processing, *Geophysics* **32**: 207-224.

Rizzini, A., Vezzani, F., Cococcetta, V. and **Milad, G.** (1976) Stratigraphy and Sedimentation of Neogene-Quaternary section in the Nile Delta area, A.R. Egypt, *presented at the Fifth Exploration Seminar at EGPC Cairo, Nov. 15-17.*

Schramm, M.W., Dedman, E.V. and **Lindsey, J.P.** (1977) *Practical Stratigraphic Modelling and Interpretation-seismic Stratigraphy*, American Ass. of Petroleum Geologist Publication.

Sheriff, R.E. (1975) Factors affecting seismic amplitudes, *Geophysical Prospecting*, **23**: 125-238.

Tatham, R.M. and **Stoffa, P.L.** (1976) V_p/V_s: a potential hydrocarbon indicator, *Geophysics* **41**: 837-849.

(Received 26/11/1983;
in revised form 24/12/1984)

تحديد الخزان في حقل أبو ماضي للغازات (دلتا النيل) باستخدام الطريقة السيزمية المعكوسة

يحيى السيد عبدالهادي

جامعة أم القرى - المملكة العربية السعودية

تعتبر الطريقة السيزمية المعكوسة من الأساليب الجديدة في التنقيب الجيوفيزيائي. وهذا البحث يناقش أساليب هذه الطريقة مع تطبيقها على مشكلة خاصة بالتنقيب عن الهيدروكربونات. فلقد طبقت الطريقة السيزمية المعكوسة على المساحات السيزمية الرقمية الحديثة في حقل أبو ماضي للغازات (مصر) في محاولة لتحديد الخزانات في هذا الحقل والحد الأمثل لتطويرها.

لقد وجد أن العدسات القليلة السمك الممتلئة بالغازات تتميز بالموجات السيزمية ذات التردد المرتفع والسعة العالية أيضا، بينما الترددات المنخفضة والسعات العالية تميز عدسات الرمل كبيرة السُّمك. ان قطاعات معالجة المويجات أوضحت بأن تكوين أبو ماضي يتميز بالتغير الجانبي للسحن الصخرية والتي ترجع الى بيئات الترسيب النهرية - الدلتية لهذه الصخور وكذلك أظهرت أن سعات الشواذ التي تميز مصادر الهيدروكربونات تمتد حتى مستويات أعمق مما كان متعارف عليه (سيدي سالم) وعلى ذلك الحفر الأعمق سوف يؤدي الى اكتشاف خزانات جديدة للغازات وللتجمعات المتكثفة.

ودراسة تحليلات السرعة التفصيلية من البيانات السيزمية أعطتنا منحنيات سرعات ذات درجة ثبات مرتفعة، ولقد أكدت من خلال نتائج وملاحظات السرعات في الآبار.

هذا دليل على أن الاستراتجرافيا الصخرية لقطاع أبو ماضي الرسوبي غير متجانس.

ومن المتوقع أن البيانات السيزمية المجمعة بواسطة معاملات حقلية واحدة مع زيادة المحتوى من الترددات العالية سوف تمدنا بنتائج أكثر فائدة.